Applicability of the Bulk-Transfer Approach to Estimate Evapotranspiration from Boreal Peatlands

PIERRE-ERIK ISABELLE*

Centre Eau Terre Environnement, Institut National de la Recherche Scientifique, Québec, Québec, Canada

DANIEL F. NADEAU

Department of Civil, Geological and Mining Engineering, Polytechnique Montréal, Montréal, Québec, Canada

ALAIN N. ROUSSEAU

Centre Eau Terre Environnement, Institut National de la Recherche Scientifique, Québec, Québec, Canada

CAROLE COURSOLLE AND HANK A. MARGOLIS

Centre d'Étude de la Forêt, Faculté de Foresterie, de Géographie et de Géomatique, Université Laval, Québec, Québec, Canada

(Manuscript received 8 September 2014, in final form 26 March 2015)

ABSTRACT

In northern landscapes, peatlands are widespread and their hydrological processes are complex. Furthermore, they are typically remote, limiting the amount and accuracy of in situ measurements. This is especially the case for evapotranspiration ET, which strongly influences watershed hydrology. The objective of this paper is to demonstrate the validity of the bulk-transfer approach to estimate ET over boreal peatlands. The simplicity of the model relies on four assumptions: (i) near-neutral atmospheric conditions; (ii) wet surface; (iii) constant momentum roughness length depending on vegetation height; and (iv) constant water vapor roughness length, with the last two assumptions implying a constant water vapor transfer coefficient C_E. Using eddy covariance data from three Canadian peatlands—Necopastic (James Bay, Québec), Mer Bleue (Ottawa, Ontario), and Western Peatland (Athabasca, Alberta)—this paper shows that these sites are characterized by frequent occurrences of near-neutral atmospheric conditions, especially the Necopastic site, with nearly 76% of the 30-min data segments occurring under near-neutral stratification. The analysis suggests these near-neutral conditions occur as a result of strong mechanical turbulence and weak buoyancy effects. The bulk-transfer approach gives promising results for 30-min and daily ET in terms of mean error and correlation, with performances similar to the Penman equation, without requiring net radiation data. The accuracy of the approach is likely related to the number of near-neutral periods and the elevated position of the water table, which backs up the wet surface assumption.

1. Introduction

Peatlands account for 3.08 million km^2 or 10%–20% of the circumpolar boreal biome (Aselmann and Crutzen 1989; Paavilainen and Päivänen 1995). Despite their widespread occurrence, they are typically found in remote areas, making their study difficult and costly. The water budgets of boreal peatlands are of great importance to accurately model regional hydrological processes in northern countries such as Canada, Finland, and Russia. To model water budgets, a precise estimate of evapotranspiration ET is essential, as it links water and energy budgets through latent heat fluxes and can account for up to 65% of annual precipitation in boreal regions (Verry 1988). The ET can be measured directly with the eddy covariance technique, considered as one of the most reliable and accurate methods (Itier and Brunet 1996). Unfortunately, eddy

* Current affiliation: Département de génie civil et de génie des eaux, Université Laval, Québec, Québec, Canada.

Corresponding author address: Pierre-Erik Isabelle, Département de génie civil et de génie des eaux, Université Laval, 1065 av. de la Médecine, Québec, QC G1V 0A6, Canada.
E-mail: pierre-erik.isabelle.1@ulaval.ca

DOI: 10.1175/JHM-D-14-0171.1

covariance towers are costly, and thus, most of the available meteorological data over boreal peatlands come from basic weather stations. Therefore, reliable methods to estimate ET have to be developed, but this is a challenging task given both the lack of data and the complex nature of peatlands.

Previous studies have identified several unique peatland features affecting ET. This type of wetland is composed mainly of organic matter, characterized by a much higher porosity (80%–90% for undecomposed peat) than mineral soil (30%–65%) (Paavilainen and Päivänen 1995). This attribute of peat soils is the result of the presence of large and well-drained macropores (Baird 1997; Silins and Rothwell 1998; Schwärzel et al. 2002; Dimitrov et al. 2010a) inducing greater air permeability (Dullien 1991). The ET could be increased by internal air circulation and convective heat exchanges in the peat fiber (Ingham and Pop 2002; Nield and Bejan 2006). On the other hand, it may be decreased by reduction of the peat water content through macropore drainage (Dimitrov et al. 2010b). A shallow water-table depth is typical of wetlands (Bailey et al. 1997), suggesting that ET will tend to be more energy limited than water limited (Price 1991; Williams et al. 2012). In addition, peatland vegetation consists of site-specific combinations of vascular (sedges, scrubs) and nonvascular (mosses) plants (Humphreys et al. 2006). In moss-dominated peatlands, the abundance of water tends to induce ET rates similar to those of open-water conditions (Kim and Verma 1996; Brümmer et al. 2012), while the presence of vascular plants modulates ET significantly through stomatal resistance (Kim and Verma 1996; Kellner 2001; Shimoyama et al. 2004; Humphreys et al. 2006; Petrone et al. 2007; Parmentier et al. 2009; Brümmer et al. 2012). Peatlands are also characterized by a unique thermal regime greatly influenced by the aforementioned features (Petrone et al. 2004; Weiss et al. 2006; Dimitrov et al. 2010a; Dissanayaka et al. 2012). Namely, the microtopography depicted by the presence of hummocks and hollows induces significant spatial heterogeneity in peat temperatures (Dimitrov et al. 2010a). For instance, the peat temperature in hummocks varies more rapidly than in hollows. This is primarily caused by conductive heat transfer from the top and the exposed sides. The high porosity ensures that convective heat transfer within the peat medium is important as well (Dimitrov et al. 2010a). Soil moisture and, indirectly, water-table depth also play a critical role for soil thermal conductivity and heat capacity. However, the impacts of this thermal regime on ET are not well known.

Previous studies used several different ET models for peatlands. Kellner (2001) stated that an energy balance approach like the Priestley and Taylor (1972) equation is very efficient for estimating ET from such surfaces. In fact, this model is the most widely used over peatlands (Kellner 2001; Petrone et al. 2004, 2007; Admiral et al. 2006; Humphreys et al. 2006; Parmentier et al. 2009; Sonnentag et al. 2010; Brümmer et al. 2012; Runkle et al. 2014). Other formulations based on the energy budget like the Penman (1948) and Penman–Monteith (Monteith 1965) equations are also commonly used (Koerselman and Beltman 1988; Campbell and Williamson 1997; Lafleur et al. 2005; Schwärzel et al. 2006; Wu et al. 2010). Despite their proven efficiency, their net radiation data requirements make them less suitable for the remote boreal peatlands, as ground-based measurements of this variable are rarely available. This is especially true since remote sensing data of net radiation are not easy to use for practical hydrological applications because of their infrequent coverage (biweekly or less when clouds are present; Kleissl et al. 2009). Also, determining net radiation with basic meteorological data is quite challenging and is likely to introduce additional uncertainties (Archibald and Walter 2014). A possible alternative to estimate ET is the simplified bulk-transfer approach (Brutsaert 2005), which is based on the equations of the Monin–Obukhov similarity theory (MOST) for momentum and water vapor profiles under near-neutral conditions, wet surfaces, and fixed roughness parameters. This approach is typically used for open-water surfaces (Fairall et al. 1996; Omstedt et al. 1997; Tanny et al. 2008); however, the relatively wet surface conditions characterizing boreal peatlands seem to place them in the applicability range of the model. Some studies have previously used the bulk-transfer approach on peatlands as a means to parameterize the surface roughness, but not for ET estimation (Shimoyama et al. 2004; Raddatz et al. 2009).

The main goal of this study was to demonstrate the usefulness of the bulk-transfer approach for ET estimation over wet boreal peatlands. After a thorough derivation of the bulk-transfer approach, this paper describes the atmospheric stratification over three boreal peatlands, showing the frequent occurrence of near-neutral atmospheric conditions and suggesting a few hypotheses explaining this peculiar behavior. A quantification of the uncertainties associated with the bulk-transfer approach follows: namely, we demonstrate that boreal peatlands seem to fall in the applicability range of the bulk-transfer approach. A comparison is then made between the modeling results and observations obtained with the eddy covariance method, along with other common ET models. The entire analysis is based on original field data collected over a boreal bog (Necopastic) and supported by flux data from two other sites (Mer Bleue and Western Peatland) in Canada.

2. Background

a. Monin–Obukhov similarity theory

The model used in this paper relies on the MOST, which states that turbulence characteristics organized into dimensionless groups should strictly depend on only a few scaling variables (Monin and Yaglom 1971). The theory applies to the inertial sublayer of the atmospheric surface layer (Stull 1988). According to MOST, wind speed and water vapor profiles can be expressed as (Brutsaert 1982)

$$\overline{u} = \frac{u_*}{\kappa}\left[\ln\left(\frac{z_m - d_0}{z_{0m}}\right) - \Psi_m\left(\frac{z_m - d_0}{L}\right) + \Psi_m\left(\frac{z_{0m}}{L}\right)\right] \tag{1}$$

and

$$\overline{q_{\rm sfc}} - \overline{q} = \frac{E}{\kappa\rho u_*}\left[\ln\left(\frac{z_v - d_0}{z_{0v}}\right) - \Psi_v\left(\frac{z_v - d_0}{L}\right) + \Psi_v\left(\frac{z_{0v}}{L}\right)\right], \tag{2}$$

where $\overline{u}$ ($\mathrm{m\,s^{-1}}$) is the mean wind velocity measured at height z_m (m); $\overline{q}$ ($\mathrm{kg\,kg^{-1}}$) is the mean specific humidity measured at height z_v (m); $\overline{q_{\rm sfc}}$ ($\mathrm{kg\,kg^{-1}}$) is the mean specific humidity evaluated just above the surface; κ is the von Kármán constant (=0.4); z_{0m} and z_{0v} (m) are the roughness lengths for momentum and humidity, respectively; d_0 (m) is the zero-plane displacement height; u_* ($\mathrm{m\,s^{-1}}$) is the friction velocity; E ($\mathrm{kg\,m^{-2}\,s^{-1}}$) is the water vapor flux; ρ ($\mathrm{kg\,m^{-3}}$) is the humid air density; Ψ_m and Ψ_v are the stability correction functions for momentum and water vapor, respectively [see Brutsaert (1982) for a complete description]; and L (m) is the Obukhov length, which is calculated as follows (Stull 1988):

$$L = \frac{-u_*^3 T_a}{\kappa g\left(\dfrac{H}{\rho c_p} + 0.61\dfrac{E}{\rho}\right)}, \tag{3}$$

where T_a (K) is the air temperature, H ($\mathrm{W\,m^{-2}}$) is the sensible heat flux, g ($\mathrm{m\,s^{-2}}$) is the gravitational constant, and c_p [J (kg K)$^{-1}$] is the specific heat of moist air. The Obukhov length cannot be measured directly by a basic meteorological station, but it can be approximated with an iterative approach (e.g., Pagowski 2006). The latter is not guaranteed to converge to the proper solution, and as such, additional uncertainties can be introduced. Nonetheless, near-neutral conditions simplify Eqs. (1) and (2), negating the necessity to calculate the Obukhov length. This study will show that such near-neutral conditions are frequent over wet boreal peatlands (section 4a), and thus, they alleviate the need to evaluate L.

b. Bulk-transfer approach

Under near-neutral conditions ($z/L \approx 0$), the stability correction terms vanish, that is $\Psi_m(0) = \Psi_v(0) \approx 0$. Therefore, Eqs. (1) and (2) can be simplified as follows:

$$u_* = \frac{\kappa\overline{u}}{\ln\left(\dfrac{z_m - d_0}{z_{0m}}\right)} \tag{4}$$

and

$$E = \frac{\kappa\rho u_*(\overline{q_{\rm sfc}} - \overline{q})}{\ln\left(\dfrac{z_v - d_0}{z_{0v}}\right)}, \tag{5}$$

and when replacing u_* in Eq.(5) with Eq.(4), E becomes

$$E = \frac{\kappa^2\rho\overline{u}(\overline{q_{\rm sfc}} - \overline{q})}{\ln\left(\dfrac{z_v - d_0}{z_{0v}}\right)\ln\left(\dfrac{z_m - d_0}{z_{0m}}\right)}. \tag{6}$$

This formulation is equivalent to the bulk-transfer approach described by Brutsaert (2005):

$$E_{\rm BT} = C_E\rho\overline{u}(\overline{q_{\rm sfc}} - \overline{q}), \tag{7}$$

where C_E is the Dalton number, a water vapor transfer coefficient that can be determined empirically, or theoretically as follows:

$$C_E = \frac{\kappa^2}{\ln\left(\dfrac{z_v - d_0}{z_{0v}}\right)\ln\left(\dfrac{z_m - d_0}{z_{0m}}\right)}. \tag{8}$$

Equation (7) requires surface specific humidity values, which is not a simple variable to obtain in practice. Therefore, the bulk-transfer formulation is more commonly used over free-water bodies (Heikinheimo et al. 1999). Over a wet surface, such as boreal peatlands with a shallow water table, $\overline{q_{\rm sfc}}$ can be approximated as the saturation value at the given surface temperature $T_{\rm sfc}$:

$$\overline{q_{\rm sfc}} = \frac{0.622}{\dfrac{p}{e_s(T_{\rm sfc})} - 0.378}, \tag{9}$$

where p (Pa) is the atmospheric pressure and $e_s(T_{\rm sfc})$ (Pa) is the saturated water vapor pressure at the surface temperature. This study will also assume a wet surface for boreal peatlands. The appropriateness of such a hypothesis will be tested in section 4b. The bulk-transfer approach has the advantage of being very simple in application if C_E is considered constant, that is, when the roughness parameters are invariant and the atmosphere

is under neutral stability. In fact, several experimental studies determined that the Dalton number can be taken as constant over oceans, with a typical value of $C_E = (1.2 \pm 0.3) \times 10^{-3}$ for a measurement height of 10 m (Brutsaert 2005). This study will also show that a constant Dalton number over boreal peatlands is not an unreasonable hypothesis (see section 4b), rendering the bulk-transfer approach useable.

3. Methods

a. Bulk-transfer modeling hypotheses

For the bulk-transfer approach to be applicable over peatlands, the three following assumptions are made: (i) near-neutral conditions are assumed time invariant; (ii) the peat surface is constantly saturated; and (iii) the momentum roughness length is constant and given by $z_{0m} = h_0/10$, where h_0 is the mean vegetation height whereas the zero-plane displacement height is also constant and given by $d_0 = 2h_0/3$. The justification behind each hypothesis and an error analysis are carefully assessed in section 4b.

The last parameter to evaluate is the water vapor roughness length z_{0v}, often quantified through the following dimensionless number:

$$\kappa B_v^{-1} = \ln\left(\frac{z_{0m}}{z_{0v}}\right), \tag{10}$$

where κB_v^{-1} is a parameter expressing the excess resistance of the air to humidity transfer with respect to the air resistance to momentum transfer. It can be either estimated from values found in the literature, optimized if direct ET measurements are available, or calculated as a function of the friction Reynolds number $\mathrm{Re}_* = u_* z_{0m}/\nu$, where ν ($\mathrm{m^2\,s^{-1}}$) is the kinematic viscosity of the air. Examples of such functions are available in Brutsaert (1982), whereas Mölder and Kellner (2002) found an optimized function for a Swedish bog ($\kappa B_v^{-1} = 1.58\mathrm{Re}_* - 3.4$). Several of these formulations were previously tested at all field sites of this study, but a fixed optimized value of κB_v^{-1} gave similar results (Isabelle 2014) and is therefore prioritized here for simplicity. That is to say that a constant water vapor transfer coefficient C_E is assumed. The optimization was performed by incrementally varying κB_v^{-1} from 0 to 30 and calculating the associated ET time series. The optimized κB_v^{-1} value was taken as the one with which a linear regression passing through the origin was along the 1:1 line with the observations. These values of κB_v^{-1} are listed in Table 3 (described in greater detail below) for each site.

Using this strategy, only five meteorological variables are needed to run the model: wind speed, surface temperature, air temperature, atmospheric pressure, and relative humidity. The model also requires various measurement heights as well as an average vegetation height, all of them considered constant.

b. Field sites and instrumentation

The main experimental site is a boreal ombrotrophic bog (Fig. 1b) named Necopastic after the nearby river, a tributary to La Grande River. It is located in the James Bay lowlands, northern Québec, Canada (53°40′28″N, 78°10′14″W; elevation is 71 m MSL and area is 0.6 $\mathrm{km^2}$). The site is mostly covered with *Sphagnum* mosses, lichens, and shrubs and is surrounded by black spruce trees, 6–8 m tall [see Nadeau et al. (2013b) for more details]. The region is characterized by a subarctic climate largely controlled by the nearby James Bay, with a mean annual temperature of −2.4°C and mean annual precipitation of 697 mm. The eddy covariance setup consisted of a 6-m flux tower with a three-dimensional sonic anemometer (CSAT3, Campbell Scientific, United States) equipped with a fine wire thermocouple and an open-path CO_2/H_2O gas analyzer (LI-7500, LI-COR Biosciences, United States). A net radiometer (CNR1, Kipp and Zonen, the Netherlands) monitored solar and terrestrial radiation, while an infrared radiometer (SI-111, Apogee Instruments, United States) measured surface temperature. Ground heat flux was measured with soil heat flux plates (HFT3, Campbell Scientific, United States) and their measurements were verified with the calorimetric method (Halliwell and Rouse 1987; Ochsner et al. 2007). The tower also featured various basic weather instruments to monitor wind speed ($z_m = 4.5$ m), air temperature, and humidity ($z_v = 5.5$ m) at several levels and air pressure. A complete description of the experimental setup can be found in Nadeau et al. (2013b).

Field measurements from two other boreal peatlands with contrasting climates were also included in the analysis. Raw data for the two sites were obtained from the FLUXNET-Canada Data Information System. The first field site is the Mer Bleue bog near Ottawa, Ontario, Canada (45°24′34″N, 75°31′7″W; elevation is 70 m MSL and area is 28 $\mathrm{km^2}$), a typical raised ombrotrophic bog (Fig. 1c), covered with *Sphagnum* mosses and shrubs [see Roulet et al. (2007) for more details]. The area is characterized by a cold, humid, continental climate with a mean annual temperature of 5.8°C and mean annual precipitation of 910 mm (Fraser et al. 2001). The experimental setup included an 8-m tower equipped with a three-dimensional sonic anemometer (1012R2 Solent, Gill Instruments, United Kingdom) and a closed-path gas analyzer (IRGA, model 6262, LI-COR Biosciences, United States), along with various other meteorological instruments ($z_m = z_v = 2$ m) (see Lafleur et al. 2003).

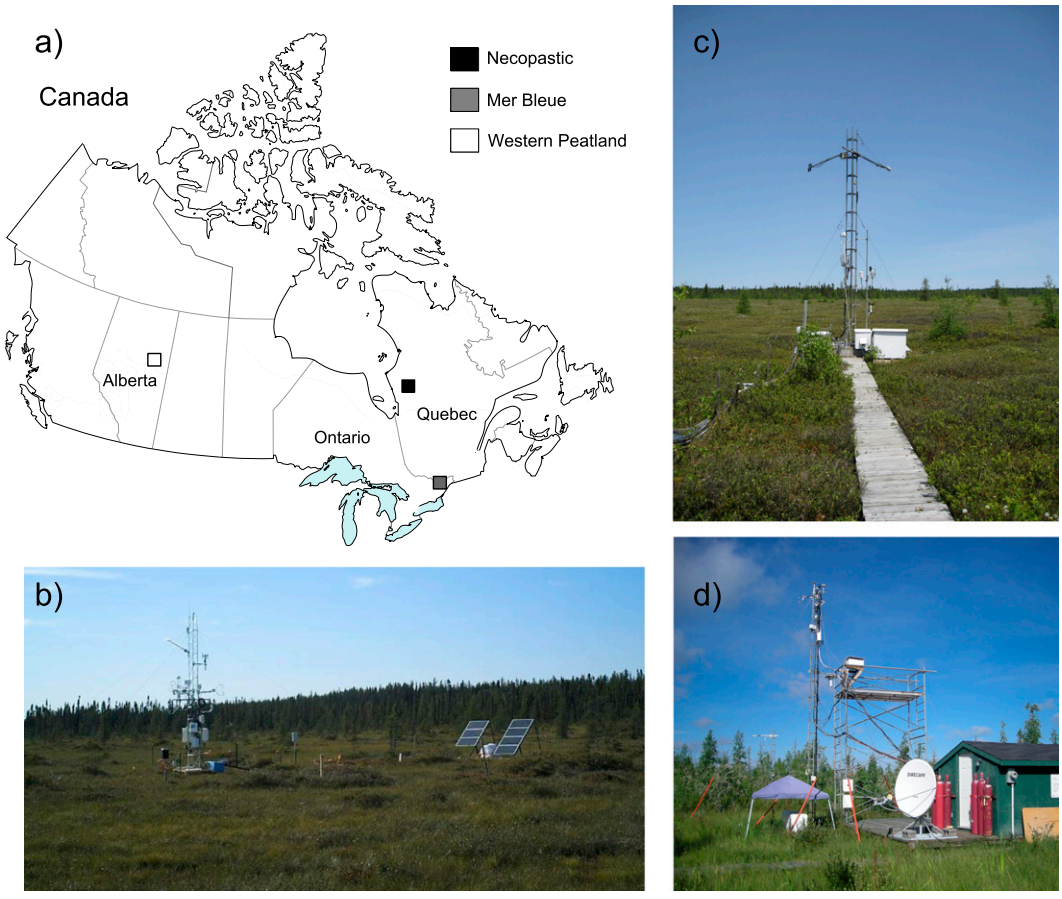

FIG. 1. (a) Location of the three study sites in Canada, (b) Necopastic (22 Jul 2012), (c) Mer Bleue (11 Jun 2011; source: Elyn R. Humphreys), and (d) Western Peatland (July 2007; source: Lawrence B. Flanagan).

The second FLUXNET-Canada site is the Western Peatland site near Lac la Biche, Alberta, Canada (54°57′14″N, 112°28′1″W; elevation is 540 m MSL and area is 10 km^2). It is a treed fen (Fig. 1d) covered with a combination of *Sphagnum*, *Aulocomnium*, and brown mosses, as well as shrubs and approximately 6-m tall trees [black spruce and larch; see Syed et al. (2006) for more details]. The Western Peatland site is characterized by a dry continental climate typical of the Canadian Great Plains, with a mean annual temperature of 2.1°C and mean annual precipitation of 504 mm (Flanagan and Syed 2011). The eddy covariance setup consisted of a three-dimensional sonic anemometer (SAT Solent R3, Gill Instruments, United Kingdom) and a closed-path gas analyzer (LI-7000, LI-COR Biosciences, United States) mounted on a 9-m flux tower, again with additional basic weather instruments ($z_m = 9.3$ m; $z_v = 4.5$ m) (see Flanagan and Syed 2011).

c. *Data processing*

Turbulent fluxes of heat, momentum, and water vapor over the Necopastic bog were computed using EddyPro, version 5.0 (LI-COR Biosciences, United States), an open-source software designed to process eddy covariance data. The precise data processing is described in Nadeau et al. (2013b). Data runs with winds blowing from a 120° sector centered on the back of the main sonic anemometer were excluded from the analysis as they were in the wake of the tower structure. Data segments with poor flux quality according to the criteria described in Mauder and Foken (2011) as well as during rainfall events were also discarded from the analysis, along with 30-min periods where the average friction velocity was under 0.2 m s^{-1}. To obtain a continuous flux time series, gap filling was performed following a standard FLUXNET approach (see Falge et al. 2001), that is, small gaps were filled by linear interpolation and large gaps were filled using marginal distribution sampling as described in Reichstein et al. (2005). The data processing for the Mer Bleue and Western Peatland followed the FLUXNET-Canada protocol (Amiro et al. 2006), while the filtering and gap filling was performed using the aforementioned method. Note that the very strict data filtering

procedure removed 46%, 28%, and 43% of the data points for the Necopastic, Mer Bleue, and Western Peatland sites, respectively.

The averaging period for the ET fluxes was 30 min and was determined using an Ogive plots analysis. The observations were collected over a full summer at the Necopastic site, that is, from 24 June to 27 September 2012. For consistency, only summer observations (from 20 June to 20 September) at the two other sites were analyzed. Their data spanned a much longer period; at Mer Bleue five summers (1999–2003) were included in the analysis, while at the Western Peatland site seven summers (2003–09) were analyzed. Those multiple summers were added to the analysis to test the bulk-transfer approach on the largest dataset possible.

d. Comparison models and metrics

To assess the accuracy of the bulk-transfer approach to estimate peatland ET, two other well-known formulations were calculated: the Hargreaves and Samani (1982) and Penman (1948) equations. The former requires fewer data inputs than the bulk-transfer approach and is described by

$$E_{\mathrm{HS}} = \alpha\left[2.3\frac{R_e}{L_v\rho}\sqrt{T_{\max}-T_{\min}}(T_a+17.8)\right], \quad (11)$$

where E_{HS} (mm day^{-1}) is the daily ET rate; R_e (J m^{-2}) is the total daily upwelling longwave radiation from the surface, which can be derived from surface temperature; L_v (J kg^{-1}) is the latent heat of vaporization of water; and $T_{\max}$, $T_{\min}$, and T_a (°C) are the maximum, minimum, and average daily temperatures, respectively. In Eq. (11), the term within square brackets represents potential daily ET, and thus, α is an empirical factor to adjust for actual ET. The Penman equation requires more data inputs than the bulk-transfer approach and is thus expected to perform better than these other models. It is described by the following equation:

$$E_P = \frac{\alpha}{L_v}\left[\frac{\Delta}{(\Delta+\gamma)}(R_n-G)+\frac{\gamma}{(\Delta+\gamma)}E_A\right], \quad (12)$$

where E_P (kg m^{-2} s^{-1}) is the water vapor flux; R_n (W m^{-2}) is the net radiation; G (W m^{-2}) is the ground heat flux; Δ (Pa K^{-1}) is the slope of saturation vapor pressure versus temperature curve; γ (Pa K^{-1}) is the psychrometric constant; and E_A (W m^{-2}) is the drying power of the air, defined by Katul and Parlange (1992) as

$$E_A = \frac{L_v\kappa^2\rho\overline{u}(\overline{q_*}-\overline{q})}{\ln\left(\frac{z_v-d_0}{z_{0v}}\right)\ln\left(\frac{z_m-d_0}{z_{0m}}\right)}, \quad (13)$$

where $\overline{q_*}=\overline{q_*}(T_a)$ (kg kg^{-1}) is the specific humidity of the air at saturation. Note that the analysis here relies on actual measurements of available energy (R_n-G) at all sites. The only differences between Eq. (13) and Eq. (6) is that the former uses the saturated air at height z_v and is expressed as a latent energy flux with L_v while the latter uses saturated air just above the surface and is a water vapor flux.

In the Penman equation, the left term within square brackets represents the equilibrium evaporation, and the right term accounts for air advection effects. An α coefficient is included to allow optimization with observed ET values, as done for the Hargreaves–Samani model. These coefficients are similar to that used with the Priestley–Taylor model (Priestley and Taylor 1972; Eichinger et al. 1996). Both α coefficients are thus obtained as the slope of a least squares regression with a zero-set origin between observed and modeled values. To quantify the performance of each model, the following metrics are computed: the normalized mean error NME, the coefficient of determination R^2, and the root-mean-square error RMSE.

e. Bulk-transfer error formulation

There are two main sources of uncertainty in the bulk-transfer formulation: (i) whether or not there is a near-neutral atmosphere and (ii) whether or not there is a wet surface. Since the experimental setup for each site included an eddy covariance tower, it is possible to quantify the errors associated with each assumption.

The error induced by the assumption of near-neutral stability can be obtained with the stability functions (Ψ_m; Ψ_v). If we isolate E in Eq. (2) and replace u_* with Eq. (1), we obtain E_{MOST} (kg m^{-2} s^{-1}), the ET flux that includes stability functions:

$$E_{\mathrm{MOST}} = \frac{\kappa^2\overline{u}\rho(\overline{q_{\mathrm{sfc}}}-\overline{q})}{\left[\ln\left(\frac{z_m-d_0}{z_{0m}}\right)-\Psi_m\left(\frac{z_m-d_0}{L}\right)+\Psi_m\left(\frac{z_{0m}}{L}\right)\right]\left[\ln\left(\frac{z_v-d_0}{z_{0v}}\right)-\Psi_v\left(\frac{z_v-d_0}{L}\right)+\Psi_v\left(\frac{z_{0v}}{L}\right)\right]}. \quad (14)$$

An error δ_s can then be defined as

$$\delta_s = \frac{|E_{\mathrm{MOST}} - E_{\mathrm{BT}}|}{E_{\mathrm{MOST}}}, \tag{15}$$

which can be simplified to

$$\delta_s = \frac{|S_1 - S_2|}{S_1}, \tag{16}$$

where

$$S_1 = \ln\left(\frac{z_m - d_0}{z_{0m}}\right) \ln\left(\frac{z_v - d_0}{z_{0v}}\right) \tag{17}$$

and

$$S_2 = \left[\ln\left(\frac{z_m - d_0}{z_{0m}}\right) - \Psi_m\left(\frac{z_m - d_0}{L}\right) + \Psi_m\left(\frac{z_{0m}}{L}\right)\right] \times \left[\ln\left(\frac{z_v - d_0}{z_{0v}}\right) - \Psi_v\left(\frac{z_v - d_0}{L}\right) + \Psi_v\left(\frac{z_{0v}}{L}\right)\right]. \tag{18}$$

Note that δ_s describes solely the impacts of including stability effects in the MOST equation.

In all likelihood, an error is induced by the hypothesis of a wet surface, possibly leading to an overestimation of ET. However, a comparison between an actual value and the one used in the bulk-transfer approach is not possible. Nevertheless, we can calculate a theoretical surface specific humidity $\overline{q_{\mathrm{sfc_{theo}}}}$ using the ET measured with the eddy covariances towers E_{EC} and Eq. (2):

$$\overline{q_{\mathrm{sfc_{theo}}}} = \frac{E_{\mathrm{EC}}}{\kappa u_* \rho}\left[\ln\left(\frac{z_v - d_0}{z_{0v}}\right) - \Psi_v\left(\frac{z_v - d_0}{L}\right) + \Psi_v\left(\frac{z_{0v}}{L}\right)\right] + \overline{q}. \tag{19}$$

This expression of a theoretical surface specific humidity depends on the roughness parameters (z_{0v} and d_0) adjusted empirically, which does not exclude cases when $\overline{q_{\mathrm{sfc_{theo}}}}$ is greater than saturation. As the latter situation is not plausible, these values are discarded from the analysis. The remaining values of theoretical surface specific humidity allow for the computation of an error associated with surface wetness δ_{sfc}:

$$\delta_{\mathrm{sfc}} = \frac{|E_{\mathrm{EC}} - E_{\mathrm{BT}}|}{E_{\mathrm{EC}}} = \frac{|\overline{q_{\mathrm{sfc_{theo}}}} - \overline{q_{\mathrm{sfc_{sat}}}}|}{\overline{q_{\mathrm{sfc_{theo}}}} - \overline{q}}, \tag{20}$$

where $\overline{q_{\mathrm{sfc_{sat}}}}$ is the surface specific humidity calculated with Eq. (9).

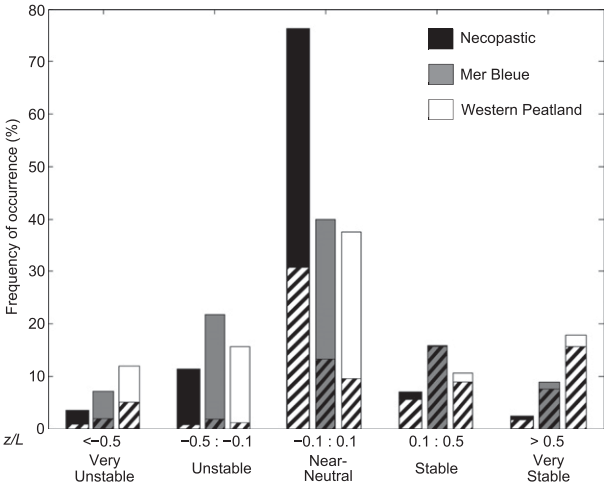

FIG. 2. Distribution of atmospheric stratification at the three sites. The striped portion of each bar represents nighttime periods (with negative net radiation).

4. Results and discussion

a. Distribution of atmospheric stability

Figure 2 shows the frequency distribution of the atmospheric stability parameter z/L, with classes of typical stability conditions and respective proportions of nighttime and daytime periods. The most remarkable feature is the recurrence of near-neutral stratification conditions defined by $|z/L| < 0.1$ at the three field sites. This threshold has been used in several other studies (Högström 1988; Mahrt et al. 2001; Novick et al. 2004; Grachev et al. 2007; Metzger et al. 2007). The Necopastic, Mer Bleue, and Western Peatland sites are under near-neutral conditions 76%, 43%, and 40% of the time, respectively, mostly during daytime. When the threshold for near-neutral stability is lowered to $|z/L| < 0.05$, these values reduce to 62%, 25%, and 26%, which is still high at the Necopastic site. These conditions are usually only observed during brief transition periods between unstable (typically daytime) and stable (typically nighttime) conditions (Stull 1988; Parlange et al. 1995), when large mechanical mixing prevails and the buoyant production or destruction of turbulence is negligible. However, frequent near-neutral conditions have been occasionally observed before over vegetated surfaces (Leclerc et al. 1990; Brunet and Irvine 2000) and urban areas (Dorsey et al. 2002; Liu et al. 2012). Complementary data from five additional sites (Table 1) allows us to compare stability conditions during the summer period for different land covers: desert playa, lakes, alpine slopes, crop fields, and boreal forests. As shown in Table 1, the frequency of occurrence of near-neutral conditions over Mer Bleue and Western Peatland does

TABLE 1. Characteristics and proportion of near-neutral periods over several surface types.

Field site	Landscape type	Measurement period	Reference	Occurrence of near-neutral conditions (%)
Necopastic Bog, Québec	Bog	From 24 Jun to 27 Sep 2012	Nadeau et al. (2013b)	76.1
West Desert, Utah	Desert playa	From 8 to 23 Jul 2002	Higgins et al. (2007)	50.8
Lake Geneva, Switzerland	Lake	From 14 Aug to 25 Oct 2006	Vercauteren et al. (2008)	44.9
Mer Bleue Bog, Ontario	Bog	Summers during 1999–2003	Lafleur et al. (2003)	42.8
Chibougamau, Canada	Mature boreal forest	Summers during 2004–10	Coursolle et al. (2012)	40.6
Western Peatland, Alberta	Forested fen	Summers during 2003–09	Flanagan and Syed (2011)	40.1
Val Ferret, Switzerland	Alpine slope	From 8 Jul to 30 Sep 2010	Nadeau et al. (2013a)	34.9
Seedorf, Switzerland	Crop field	From 5 Aug to 5 Sep 2008	Froidevaux et al. (2013)	19.5

not appear uncommon, but clearly the Necopastic site stands out.

We hypothesize that atmospheric buoyancy effects are minimized at this site due in part to the large thermal inertia of peatlands with shallow water tables. The thermal properties of peat media are largely governed by the volumetric water content (Dissanayaka et al. 2012). Indeed, the large porosity and high moisture content of the peat increases heat capacity because this property has a higher value for water (Novak and Black 1985). Saturated peatlands have also a similar thermal conductivity to that of dry mineral soils (Oke 1987). However, since they have a much greater heat storage capacity, their thermal inertia is much higher. This leads to weak daily fluctuations of surface temperatures and thus to small sensible heat exchanges, as well as weak buoyancy effects. Figure 3 presents the mean energy budget at the Necopastic site, which shows that daytime ground heat flux can take substantial values considering that net radiation has an average midday peak of $\sim 350\,\mathrm{W\,m^{-2}}$. In addition, Fig. 3 shows that when solar radiation is supplied to the surface, the large water availability favors latent heat exchange in the energy balance. As an indication, the average midday Bowen ratios have values of 0.5, 0.77, and 0.83 for the Necopastic, Mer Bleue, and Western Peatland sites, respectively. The significantly higher water-table levels at the Necopastic site (11 cm below the surface on average vs 50 and 45 cm at the Mer Bleue and Western Peatland sites, respectively) can in all likelihood explain the higher occurrences of near-neutral periods by enhancing ground and latent heat fluxes.

Near-neutral conditions can also occur when cloudy conditions prevail, as clouds reduce the available energy at the surface, thus decreasing sensible heat exchanges. The three field sites were indeed also subject to frequent nighttime fog. Guided by hourly photographs taken at the Necopastic site, the following criteria were applied to identify typical foggy conditions: (i) vapor pressure deficit under 100 Pa, (ii) net radiation fluxes between -50 and $50\,\mathrm{W\,m^{-2}}$, and (iii) wind speeds under $1.5\,\mathrm{m\,s^{-1}}$. It was found that during 67%, 82%, and 79% of the nights, fog was present for at least half of the nighttime periods at the Necopastic, Mer Bleue, and Western Peatland sites, respectively. Nighttime fog acts as an insulating layer that lessens radiative cooling at the surface, reducing the strength of the nocturnal inversion and thus reinforcing the tendency toward near-neutral stability. In fact, for the Necopastic site, under nighttime foggy conditions, 70% of the 30-min data segments were under near-neutral conditions.

In addition to weak atmospheric buoyancy effects, near-neutral conditions can only occur under a certain level of mechanical mixing, described by the friction velocity u_*. In the case of our three field sites, near-neutral conditions seem to be observed almost strictly when $u_* > 0.2\,\mathrm{m\,s^{-1}}$, even with the unfiltered data. This friction velocity threshold is met 66%, 45%, and 55% of the time at the Necopastic, Mer Bleue, and Western Peatland sites, respectively. This would seem to indicate that mechanical mixing is related to near neutrality, as expected.

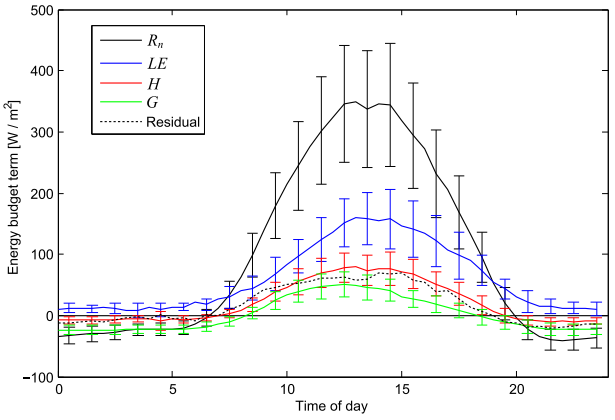

FIG. 3. Mean energy budget at the Necopastic site for the summer 2012, where R_n is the net radiation, LE is the latent heat flux, H is the sensible heat flux, G is the ground heat flux, and the residual is calculated as $R_n - \mathrm{LE} - H - G$. The error bars are the std dev of each term at every hour.

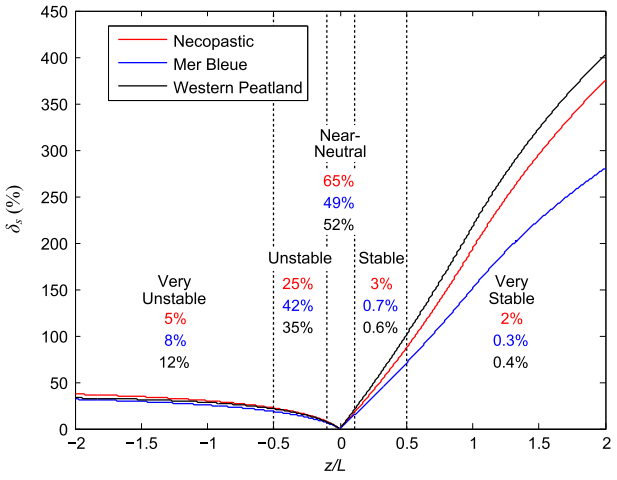

FIG. 4. Variation of δ_s as a function of the stability parameter z/L for the three sites. The percentages shown relate to the proportion of total cumulative ET measured when the atmosphere is under the specified stability class, for every field site.

b. *Error analysis on the model assumptions*

1) NEAR-NEUTRAL CONDITIONS

Near-neutral conditions are the basis behind the use of the bulk-transfer method. However, as shown in section 4a, these conditions are especially common at the Necopastic site, but not so much at the two other sites. Thus, justifying the assumption of a constant near-neutral atmosphere is critical.

Figure 4 presents the variation of δ_s [Eq. (15)] as a function of atmospheric stability for the three field sites. The shown percentages are the proportion of total cumulative ET observed under each class of atmospheric stability, for each study site, and for the whole study period. One can notice that as the atmosphere becomes more unstable, δ_s increases much more gently compared to when the atmosphere becomes more stable. For instance, the error reaches over ~300% when $z/L = 2$, while it is only ~40% when $z/L = -2$. As shown in Fig. 2, stable conditions occur mostly at night, when ET is typically very low (as shown by the proportion of total cumulative ET for the "stable" and "very stable" classes), which significantly decreases the impact of those high δ_s values from a water balance standing point. However, the same cannot be said for unstable periods typically occurring when solar radiation and ET are maximized, especially for the $-0.5 < z/L < -0.1$ stability range.

Figure 5 presents the histogram of δ_s for the three field sites between 0% and 100%, showing that it logically depends on the proportion of near-neutral periods. Small errors (0%–10%) are present for ~65% of the data segment at the Necopastic site, whereas that value drops to ~59% and ~40% for Mer Bleue and Western Peatland, respectively. The average δ_s values are 11%, 13%, and 18% and the medians are 5.3%, 7.6%, and 15.7% for Necopastic, Mer Bleue, and Western Peatland sites, respectively. If we compute the cumulative error induced on the observed ET values by the near-neutrality assumption (i.e., $\delta_s E_{EC}$) for the complete period of study, we obtain total relative errors of 13.4%, 6.4%, and 10.8% for the Necopastic, Mer Bleue, and Western Peatland sites, respectively. Therefore, assuming near neutrality at all times can potentially induce large relative errors in the estimation of short time interval ET (hourly and daily), but they become negligible on a cumulative basis (weeks, months, and seasons).

2) WET SURFACE

The assumption of a wet surface stems from a need to simplify the bulk-transfer approach since it thereby

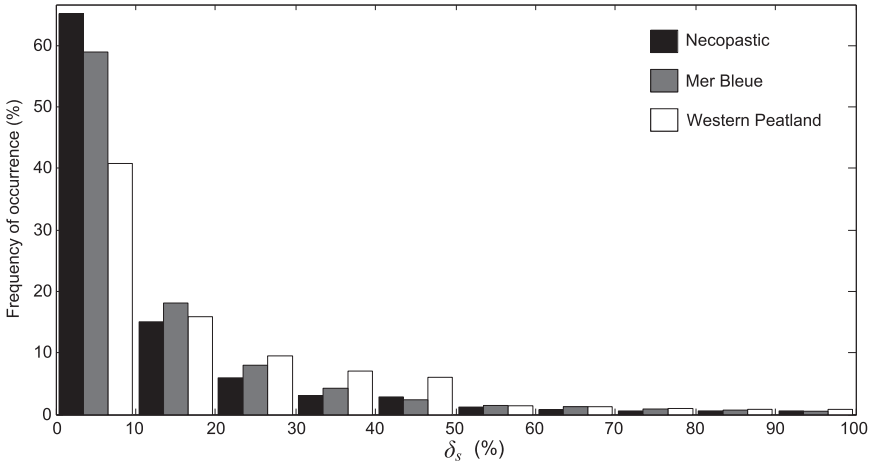

FIG. 5. Distribution of the error related to atmospheric stability δ_s for the three field sites.

cancels the dependence on surface specific humidity data. The peat surface is not always wet, especially at the Mer Bleue and Western Peatland sites, where the water table is always at least 30 cm below the surface, and sequences of several rain-free days regularly occur. However, this assumption is particularly relevant for the Necopastic site, where the water-table position varies between 3 and 18 cm below the surface. Figure 6 shows the comparison between $\overline{q_{\mathrm{sfc_{theo}}}}$ and $\overline{q_{\mathrm{sfc_{sat}}}}$ for the three field sites, along with least squares regressions for each summer studied.

The water-table position at Mer Bleue is relatively stable during the measurement period, with an average of ~54 cm below the surface, except for the summers of 2000 (~35 cm below the surface) and 2003 (~50 cm below the surface). Consequently, for these two summers, the assumption of a saturated surface induces the smallest overestimation of theoretical surface specific humidity, as shown by the gentler slopes of their respective linear regressions. A similar trend is observed for the Western Peatland site where summers from 2003 to 2005 have a relatively stable water-table level at an average of ~30 cm below the surface while an increase in depth occurs thereafter (2006, ~46 cm; 2007, ~50 cm; 2008, ~55 cm; and 2009, ~66 cm below the surface). The slopes of the linear regression lines also appear to be increasing with time. This suggests that a deeper water table is associated with a nonsaturated surface.

Figure 7 shows the distribution of δ_{sfc} at the three study sites for the interval 0%–100%. The distribution of δ_{sfc} is much wider than that of δ_s (Fig. 5). On a water balance basis, the cumulative error induced by the wet surface hypothesis (i.e., $\delta_{\mathrm{sfc}}E_{\mathrm{EC}}$) has a relative value of 26%, 29%, and 37% for the Necopastic, Mer Bleue, and Western Peatland sites, respectively, and for the whole period of study. As expected, the assumption of a wet surface is more appropriate for sites with a shallower water table. This also seems to indicate that the assumption of a wet surface is a larger source of uncertainty than the near-neutral assumption. It should be recalled that the two errors are not directly comparable. Indeed, δ_s is a comparison of the response of the Monin–Obukhov profile equations with and without the effects of atmospheric stability, whereas δ_{sfc} is a comparison of observed ET with respect to that from a saturated surface, both expressed using the bulk-transfer approach. This subtlety is important, because the latter compares modeled values with observations whereas the former does not, which may explain a larger δ_{sfc} in proportion.

In the end, the distribution of δ_{sfc} may lead to the conclusion that the hypothesis of a saturated surface is not always met. Confirmation of the rejection of this specific assumption depends essentially on direct measurements

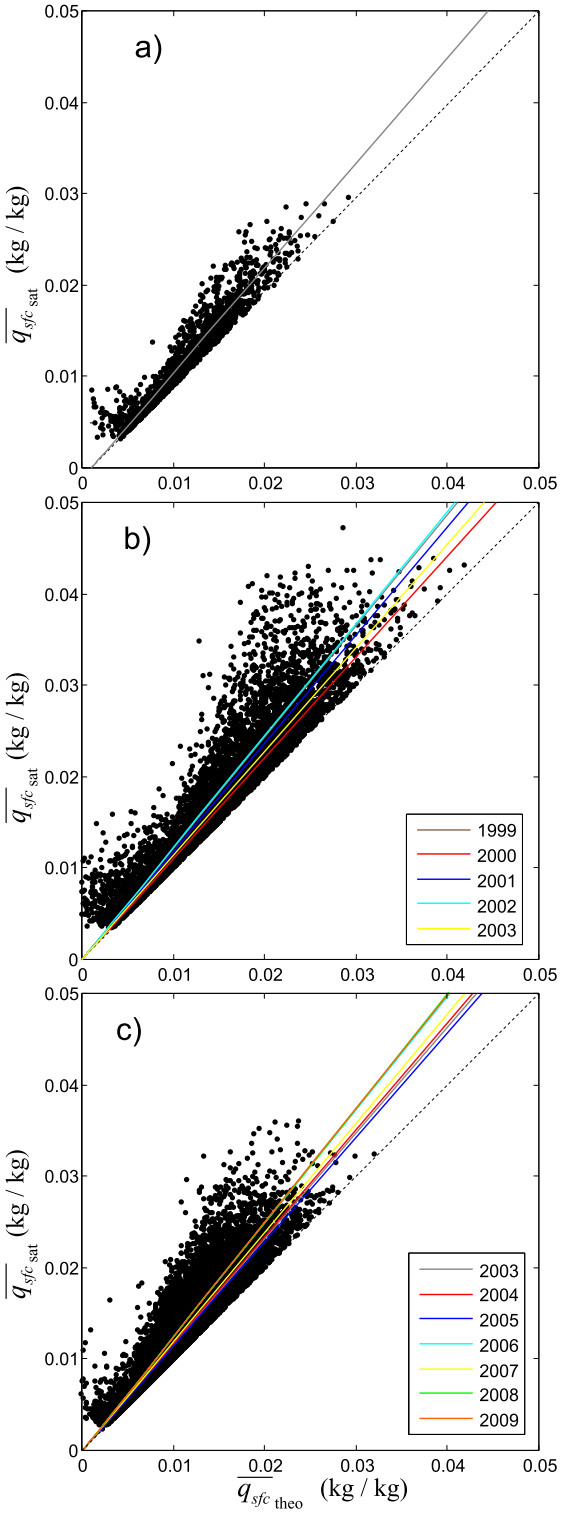

FIG. 6. Comparison of $\overline{q_{\mathrm{sfc_{theo}}}}$ and $\overline{q_{\mathrm{sfc_{sat}}}}$ for each year of study at the (a) Necopastic, (b) Mer Bleue, and (c) Western Peatland sites. The dashed line shows the cutoff at the 1:1 line, while the plain lines are linear regressions with zero-set origin for each year of study.

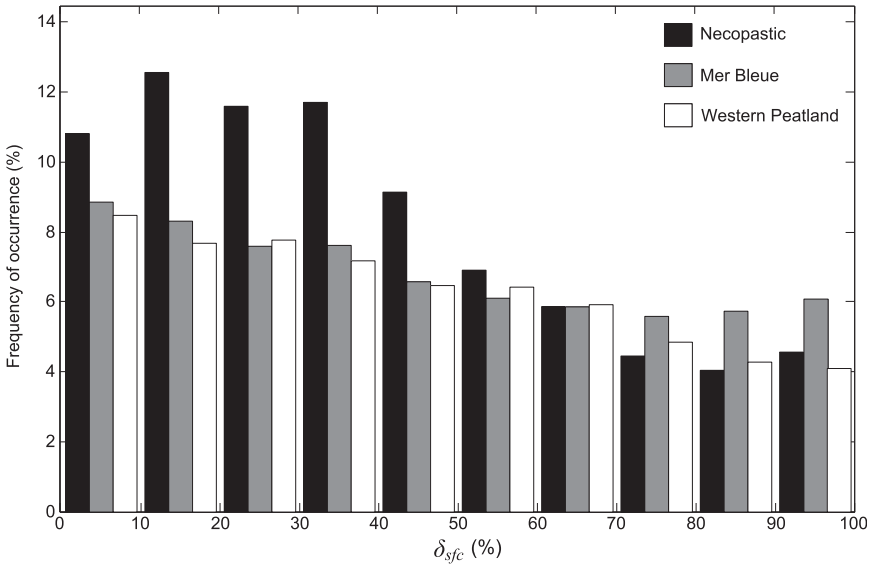

FIG. 7. Distribution of δ_{sfc} for the three field sites.

of surface humidity, which are not easy to obtain in practice.

3) MOMENTUM ROUGHNESS LENGTH

The assumption of a constant momentum roughness length z_{0m} taken as a tenth of the mean vegetation height h_0 is quite common in micrometeorology (Brutsaert 1982, 2005), but its appropriateness still needs to be assessed. A field estimate at the Necopastic site provided $h_0 \approx 0.5$ m, leading to an estimation of $z_{0m} \approx 0.05$ m. This value can be verified with Eq. (4) since the eddy covariance setup measures u_* directly. This equation also relies on the value of the zero-displacement plane height d_0, but the assumption $d_0 \approx (2/3)h_0$ is generally considered a good approximation (Brutsaert 1982). This is especially true given that the estimation of "d_0 is not as critical as that of z_{0m}" (Brutsaert 1982, p. 116).

Figure 8 presents the histogram of the values of z_{0m} along 16 wind vectors, with the numerical values of the median of z_{0m} for each direction. In the main wind direction (northwest), it takes a value close to 0.05 m. On this site, the hypothesis seems satisfactory given the advantage that it also offers in simplicity.

No mean vegetation height estimates within the measurement footprint area were available at the two FLUXNET sites. The mean vegetation height was rather obtained by an iterative optimization approach using Eq. (4) and the relations described previously. This procedure gave h_0 values of 0.32 and 4.02 m for Mer Bleue and Western Peatland, respectively. These values corroborate the relevance of the momentum roughness length assumption with respect to the description of the vegetation cover at each study site.

The main weakness of the assumption is that z_{0m} is taken as constant throughout the growing season, while it is clear that the appearance of leaves increases surface roughness. However, no clear seasonal tendency in z_{0m} could be identified.

4) WATER VAPOR ROUGHNESS LENGTH

Again, once z_{0m} is estimated, it is possible to calculate z_{0v} with Eq. (5) since u_* and E are measured with the eddy covariance tower. Figure 9 presents the wind rose histogram of z_{0v} values for the Necopastic site along 16 wind directions. In this figure, a filter based on the latent heat flux value was applied (LE $> 50\,\mathrm{W\,m^{-2}}$) to exclude outliers. This figure shows that the distribution of z_{0v} is wide, especially considering the logarithmic scale. This has been reported in several other studies (Brutsaert et al. 1990; Kotani and Sugita 2005; Moriwaki and Kanda 2006; Park et al. 2010). However, as mentioned in section 3a, the use of a constant z_{0v} value gave results similar to a varying value of the parameter function of the Reynolds number, reinforcing the appropriateness of the assumption.

c. *30-min* ET *fluxes at the Necopastic site*

Of the three sites included in this analysis, Necopastic is the one where the use of the bulk-transfer approach appears most promising. Indeed, it has the highest water table on average as well as the most frequent near-neutral conditions. As such, we attempt here to use this approach at the 30-min time scale. To do so, friction velocity is found by means of Eq. (4) and ET rates are determined with Eq. (5).

Figure 10 shows the comparison of the 30-min averaged u_* calculated with Eq. (4) and measured with the

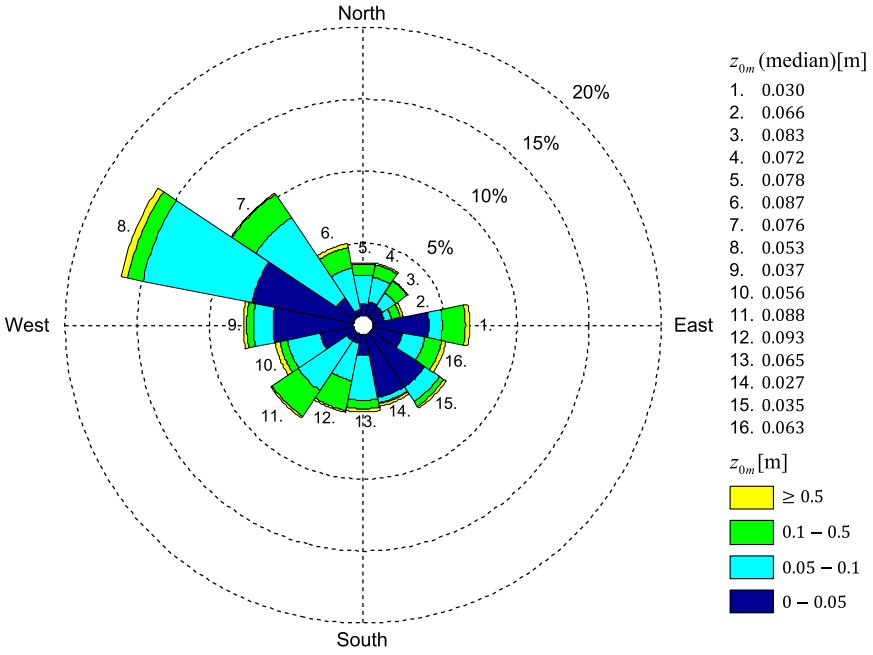

FIG. 8. Wind rose distribution of z_{0m} with the median associated with each wind direction on the Necopastic site.

eddy covariance tower. Figure 10a shows a point-by-point classification from a stability point of view, while Fig. 10b separates them on a day/night basis. Both figures show that the neutral MOST equation can describe the measured friction velocity with great accuracy, with a global NME of 15% and an R^2 of 0.84, and the worst performances occur during nonneutral periods (Table 2). As was mentioned before, when $u_* > 0.2\,\mathrm{m\,s^{-1}}$, most of the 30-min data segments are under near-neutral conditions. The day/night classification gives the same type of

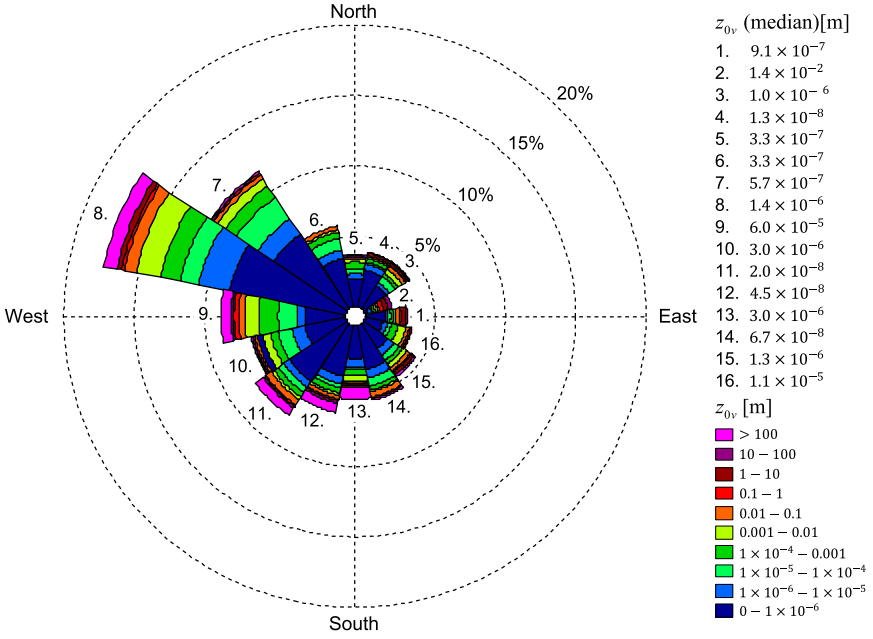

FIG. 9. Wind rose distribution of z_{0v} with the median associated with each wind direction for the Necopastic site.

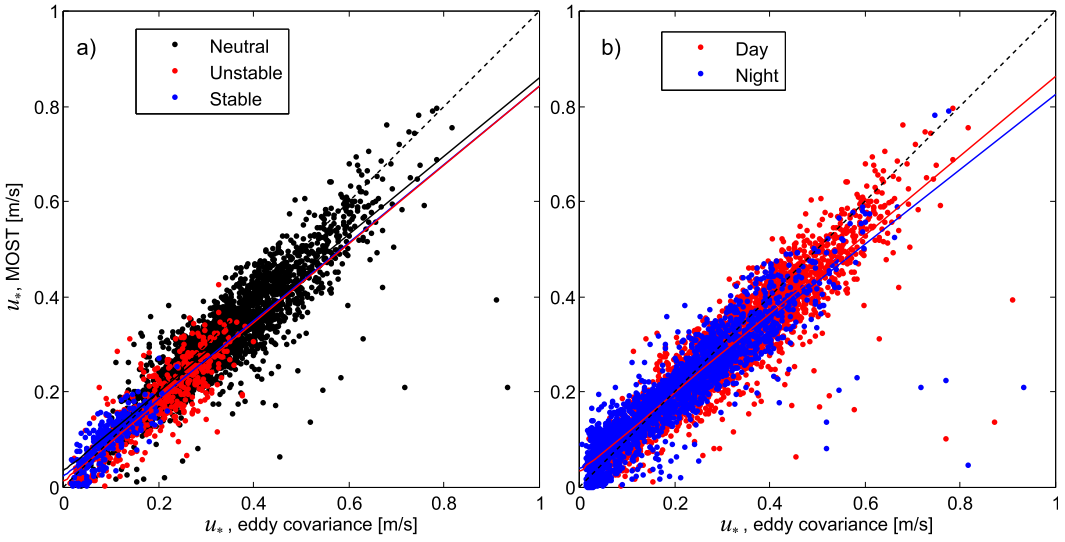

FIG. 10. Comparison of u_* measured with the eddy covariance tower and calculated with Eq. (4) on the Necopastic field site, classified by (a) stability conditions and (b) day or night. The solid lines are linear regressions of the same color points, and the dashed lines are the 1:1 lines.

accuracy, with an NME of 15% and an R^2 of 0.81, expressing the larger dependence of the model efficiency on stability conditions than solar radiation.

Similarly, Fig. 11 shows the comparison of 30-min-averaged ET rates obtained with the bulk-transfer model ($\kappa B_v^{-1} = 11$) and with measurements. As an indication, the global performances of the bulk-transfer approach at the Necopastic site are relatively satisfactory, with an NME of 44% and an R^2 of 0.74. The model performs essentially as well as the Penman equation (NME = 44%, R^2 = 0.75), which is interesting given that it does not require net radiation as an input.

The modeled ET did not agree with observations under stable stratification (Table 2). The very high NME under such conditions is probably caused by the smaller values of ET, giving more relative weight to otherwise small errors. Surprisingly, the bulk-transfer model performed best under unstable daytime stratification. This result is probably a consequence of the few 30-min periods where the bulk-transfer approach computes a low ET while the observations are not negligible (i.e., the data points along the x axis in Fig. 11a). These significant outliers have a strong influence on the computed statistics by increasing NME and decreasing R^2.

The bulk-transfer model appears to overestimate ET when observed values exceed 0.15 mm. We believe this is caused by a problem with the wet surface hypothesis. Indeed, these high ET values occur when net radiation is large and occasionally at the end of a sequence of several rain-free days, thereby suggesting that the surface was not saturated.

d. *Cumulative* ET

Side-by-side comparison of observed ET and its value computed by the bulk-transfer approach appears promising on a 30-min scale for the Necopastic site. For water budget analyses, longer time scales are needed though. Figure 12 presents the cumulative ET obtained with the eddy covariance tower, as well as that calculated with the bulk-transfer approach. The figure also features the cumulative ET from the Penman and Hargreaves–Samani equations presented in section 3d. Note that the Hargreaves–Samani curve has a smoother shape because of the fact that ET is computed on a daily basis with this model. Also, only the summer of 2003 is presented for Mer Bleue, since the Penman equation relies on net radiation data that are not available at this site for the summers of 1999–2002.

Figure 12 shows that the bulk-transfer approach performs well at estimating seasonal ET at the three field sites. The model offers a proper alternative to the Penman equation, even if the latter is generally more precise. The bulk-transfer approach generally underestimates ET in terms of total volumes. The summers of 2008 and 2009 on the Western Peatland are an exception to this

TABLE 2. Performance of the bulk-transfer approach in modeling of u_* and ET at the Necopastic site under different stability conditions, 30-min scale, $\kappa B_v^{-1} = 11$.

	u_*			ET		
Metric	Near neutral	Stable	Unstable	Near neutral	Stable	Unstable
NME	0.13	0.23	0.21	0.47	1.60	0.28
R^2	0.78	0.64	0.70	0.69	0.45	0.82

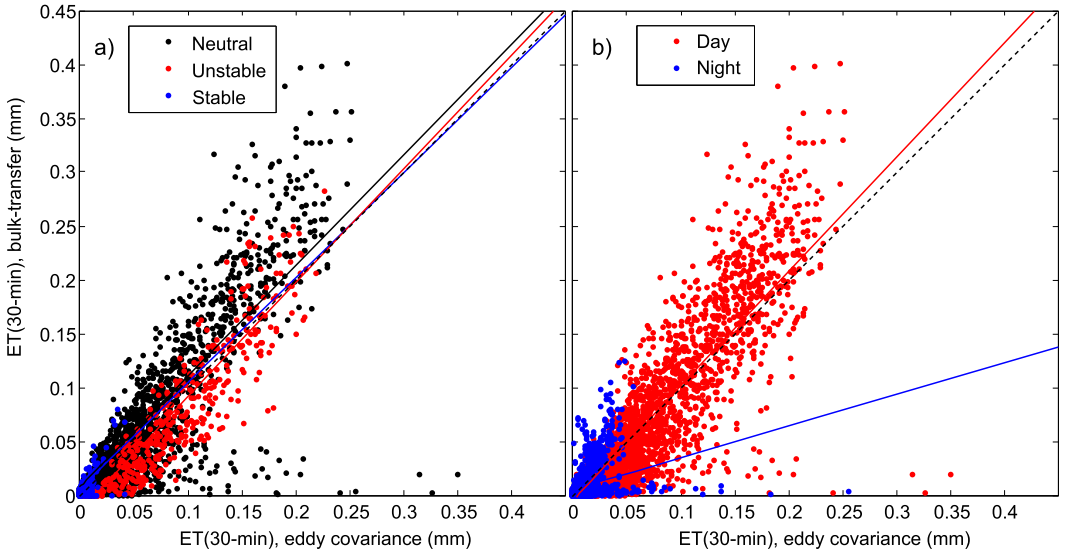

FIG. 11. Comparison of the 30-min-averaged ET measured with the eddy covariance tower and calculated with the bulk-transfer model ($\kappa B_v^{-1} = 11$) on the Necopastic field site, classified by (a) stability conditions and (b) day or night. The solid lines are linear regressions of the same color points, and the dashed lines are the 1:1 lines.

conclusion, in all likelihood caused by the very low water-table height during that period. Note that under these conditions, the Penman equation also overestimates ET.

These results seem to agree with the conclusions drawn in section 4b: the errors induced by the modeling assumptions with the bulk-transfer approach can take significant value, but they tend to become negligible on a cumulative basis.

e. *Daily* ET

Table 3 compares the daily ET obtained with each model studied along with in situ observations at every field site. The results of the bulk-transfer approach are also shown graphically in Fig. 13. In Fig. 13a, the error bars associated with the eddy covariance data (x axis) are obtained using the random uncertainty estimation (Finkelstein and Sims 2001), while those associated with the bulk-transfer model (y axis) represent a sum of the errors associated with the meteorological instruments and the time-invariant, perfectly neutral atmosphere hypothesis. The latter is taken as the difference between the ET rates given by Eq. (2) with and without the inclusion of the stability correction term Ψ. All these sources of uncertainties are obtained for every 30-min segment and then summed daily as prescribed by the uncertainty propagation principles.

The bulk-transfer approach offers a fair alternative to the Penman equation in ET estimation, with only slightly higher NME values, particularly for the Necopastic and Western Peatland sites. Evidently, with the addition of net radiation inputs, the Penman equation provides the best ET estimates regardless of the study site or the performance metric used. This was to be expected, as solar radiation is a key driver of ET. The decrease in accuracy from Necopastic to the two FLUXNET sites is probably caused by their least amount of near-neutral 30-min segments. It seems reasonable that the ability of the bulk-transfer model to predict ET is correlated to the proportion of near-neutral periods. However, even for the Mer Bleue and Western Peatland sites, the bulk-transfer approach explains a greater percentage of the data variance than the Hargreaves–Samani equation (as expressed by the higher R^2 value), despite both of them relying on the same amount of input variables.

As previously discussed, the bulk-transfer approach appears to overestimate ET when observations exceed a certain threshold (here 3 mm) at the Mer Bleue and Western Peatland sites. This behavior explains the high values of RMSE found at these two locations, as this metric is more sensitive to large errors. This is a limitation of this approach and could cause a significant ET overestimation by error accumulation.

The κB_v^{-1} values for each site were optimized with the eddy covariance data and presented in Table 3. Park et al. (2010) did an extensive survey of the typical values of κB_v^{-1} for bare soils (0–10) and a grassland (10–30). Kotani and Sugita (2005) found κB_v^{-1} to range from 7 to 34 for tall grass and from 14 to 27 for forest, whereas Brutsaert et al. (1990) found a range between 7 and 12 for a prairie. When optimized, values from the three field sites clearly lie within these ranges. The great difference in values between the Necopastic site and the two complementary

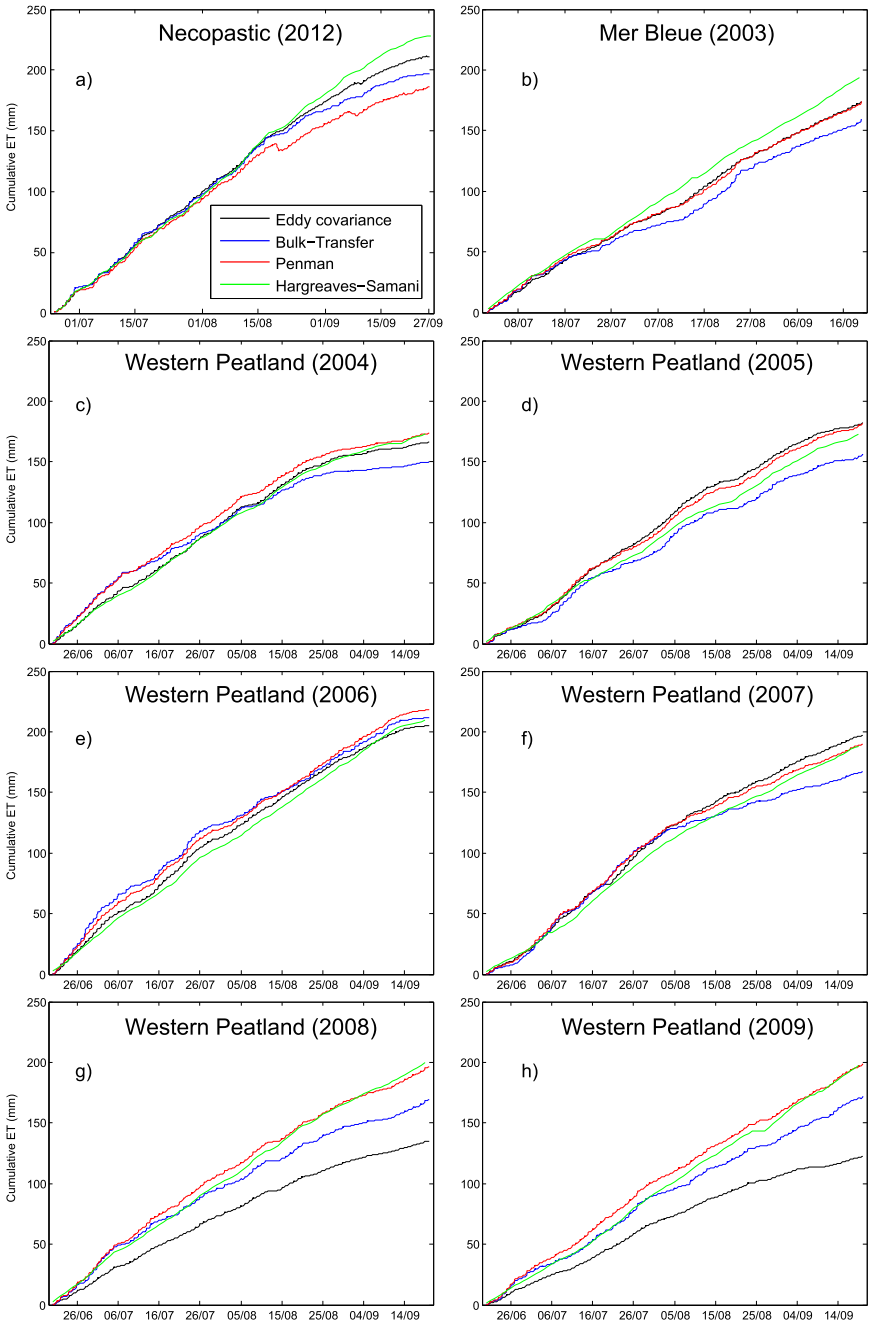

FIG. 12. Cumulative ET from eddy covariance observations, bulk-transfer approach, and Penman and Hargreaves–Samani equations. (a) Necopastic, 2012; (b) Mer Bleue, 2003; (c) Western Peatland, 2004; (d) Western Peatland, 2005; (e) Western Peatland, 2006; (f) Western Peatland, 2007; (g) Western Peatland, 2008; and (h) Western Peatland, 2009.

sites is likely an effect of the significant difference in water-table positions and vegetation cover.

5. Conclusions

The broad objective of this study was to gain a better understanding of the processes controlling daily ET over boreal peatlands in order to find a simple model valid for regions with limited data availability. The analysis was supported by eddy covariance data, originating from a field survey (Necopastic) and from the FLUXNET-Canada database (Mer Bleue and Western Peatland).

TABLE 3. General results and performance of the three models for the three sites, daily scale, and fixed and site-dependent κB_v^{-1}.

Results	Necopastic	Mer Bleue	Western Peatland
Near-neutral data segments (%)	76.1	42.8	40.1
No. of days analyzed	63	170	567
Optimized κB_v^{-1}	11.0	21.4	23.8
h_0 (m)	0.50	0.32	4.02
C_E ($\times 10^{-3}$)	2.32	1.56	2.26
α (Penman)	0.58	0.42	0.28
α (Hargreaves–Samani)	0.74	0.55	0.55
NME			
Bulk transfer	0.16	0.27	0.31
Hargreaves–Samani	0.26	0.26	0.29
Penman	0.07	0.02	0.21
R^2			
Bulk transfer	0.82	0.43	0.59
Hargreaves–Samani	0.59	0.20	0.45
Penman	0.92	0.87	0.68
RMSE (mm)			
Bulk transfer	0.55	0.85	0.75
Hargreaves–Samani	0.67	0.76	0.67
Penman	0.32	0.27	0.52

At first, a detailed description of the atmospheric stability at the three sites was performed. The latter showed the recurrence of near-neutral atmospheric conditions owing to the thermal inertia of saturated peat, the typically small Bowen ratios, and frequent cloudy conditions. These three phenomena jointly act to minimize sensible heat flux and buoyancy effects, while mechanical mixing is nonnegligible. These atmospheric conditions allow us to simplify the MOST profile equations for momentum and water vapor, conducive to the bulk-transfer approach, which turns out to be a simple yet robust means to estimate ET. To do so, four assumptions are needed: (i) time-invariant near-neutral conditions, (ii) wet surface, (iii) constant momentum roughness length dependent on vegetation height, and (iv) constant water vapor roughness length. The precision of the model is proportional to the occurrence of near-neutral periods, which seems to be linked to the position of the water table. This last connection will have to be more thoroughly investigated in future studies. Other studies are also needed to show if other boreal peatlands are characterized by frequent near-neutral conditions.

This model provides a pragmatic framework to estimate and predict ET over peatlands, a landscape that is of a high importance to hydrologists and ecologists. Considering the remoteness and vastness of these environments, especially in boreal regions where ground-based radiation data are rarely available, the simplicity and low cost of the model is a significant breakthrough for understanding the processes involved, especially in

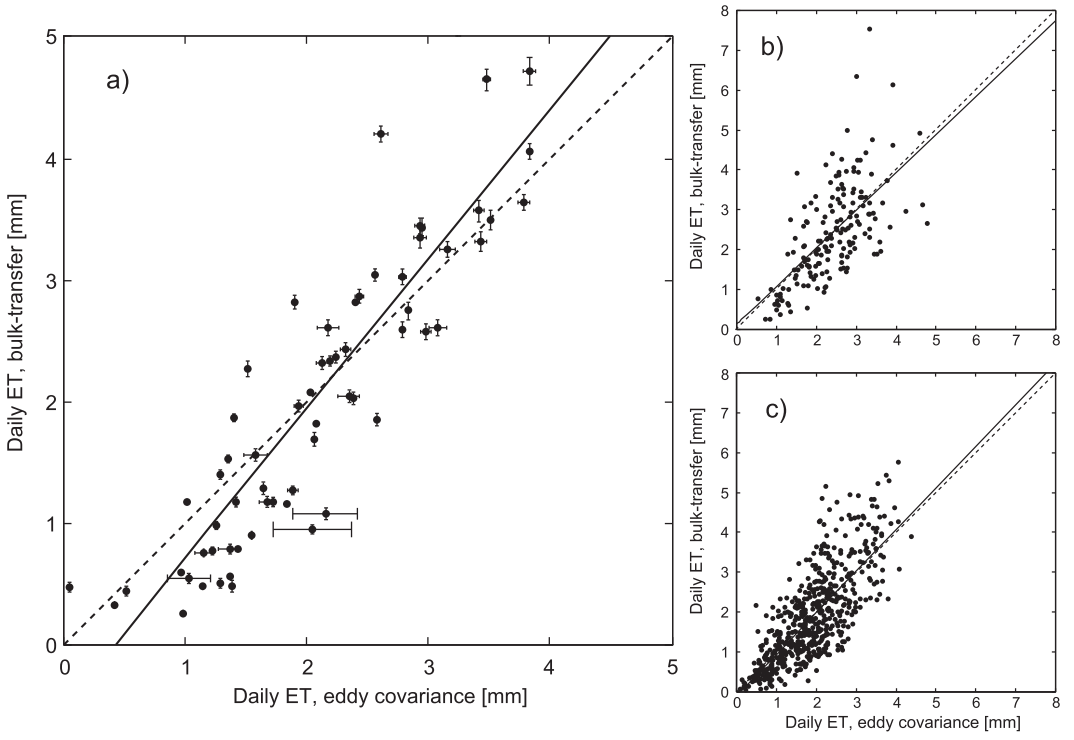

FIG. 13. Daily ET estimated with the bulk-transfer model vs eddy covariance observation at (a) Necopastic, (b) Mer Bleue, and (c) Western Peatland sites. The solid line is a linear regression of the data, and the dashed line is the 1:1 line.

an operational watershed-based hydrological context. Ultimately, the model could be applied to other types of wetlands, and even to other environments, given that near-neutral periods are frequent and that surface is wet. A next step for the model would also be to find a simple relation for the variation of C_E on a seasonal scale.

Acknowledgments. The authors thank the Cree Nation of Chisasibi as well as S. Grindat, S. Lambert-Girard, G. Carrer, G. Hould-Gosselin, M. Oreiller, M. Fossey, C. Fortier, and C. Guay for their collaboration with the field campaign. We would also like to thank FLUXNET-Canada, and particularly Peter M. Lafleur, Elyn R. Humphreys, and Lawrence B. Flanagan of the research teams of the Mer Bleue and Western Peatland sites for providing the data and valuable comments and insights. This work was supported by Ouranos (consortium on regional climatology and adaptation to climate change), the Natural Sciences and Engineering Research Council of Canada, and the Canadian Foundation for Climate and Atmospheric Sciences.

REFERENCES

Admiral, S. W., P. M. Lafleur, and N. T. Roulet, 2006: Controls on latent heat flux and energy partitioning at a peat bog in eastern Canada. *Agric. For. Meteor.,* **140,** 308–321, doi:10.1016/j.agrformet.2006.03.017.

Amiro, B. D., and Coauthors, 2006: Carbon, energy and water fluxes at mature and disturbed forest sites, Saskatchewan, Canada. *Agric. For. Meteor.,* **136,** 237–251, doi:10.1016/j.agrformet.2004.11.012.

Archibald, J. A., and M. T. Walter, 2014: Do energy-based PET models require more input data than temperature-based models? An evaluation at four humid FLUXNET sites. *J. Amer. Water Resour. Assoc.,* **50,** 497–508, doi:10.1111/jawr.12137.

Aselmann, I., and P. J. Crutzen, 1989: Global distribution of natural freshwater wetlands and rice paddies, their net primary productivity, seasonality and possible methane emissions. *J. Atmos. Chem.,* **8,** 307–358, doi:10.1007/BF00052709.

Bailey, W. G., T. R. Oke, and W. Rouse, Eds., 1997: *Surface Climates of Canada*. Canadian Association of Geographers Series in Canadian Geography, Vol. 4, McGill–Queen's Press, 400 pp.

Baird, A. J., 1997: Field estimation of macropore functioning and surface hydraulic conductivity in a fen peat. *Hydrol. Processes,* **11,** 287–295, doi:10.1002/(SICI)1099-1085(19970315)11:3<287::AID-HYP443>3.0.CO;2-L.

Brümmer, C., and Coauthors, 2012: How climate and vegetation type influence evapotranspiration and water use efficiency in Canadian forest, peatland and grassland ecosystems. *Agric. For. Meteor.,* **153,** 14–30, doi:10.1016/j.agrformet.2011.04.008.

Brunet, Y., and M. R. Irvine, 2000: The control of coherent eddies in vegetation canopies: Streamwise structure spacing, canopy shear scale and atmospheric stability. *Bound.-Layer Meteor.,* **94,** 139–163, doi:10.1023/A:1002406616227.

Brutsaert, W., 1982: *Evaporation into the Atmosphere: Theory, History, and Applications*. D. Reidel, 299 pp.

——, 2005: *Hydrology: An Introduction*. Cambridge University Press, 605 pp.

——, M. Sugita, and L. J. Fritschen, 1990: Inner region humidity characteristics of the neutral boundary layer over prairie terrain. *Water Resour. Res.,* **26,** 2931–2936, doi:10.1029/WR026i012p02931.

Campbell, D. I., and J. Williamson, 1997: Evaporation from a raised peat bog. *J. Hydrol.,* **193,** 142–160, doi:10.1016/S0022-1694(96)03149-6.

Coursolle, C., M.-A. Giasson, H. A. Margolis, and P. Y. Bernier, 2012: Moving towards carbon neutrality: CO_2 exchange of a black spruce forest ecosystem during the first 10 years of recovery after harvest. *Can. J. For. Res.,* **42,** 1908–1918, doi:10.1139/x2012-133.

Dimitrov, D. D., R. F. Grant, P. M. Lafleur, and E. R. Humphreys, 2010a: Modeling peat thermal regime of an ombrotrophic peatland with hummock–hollow microtopography. *Soil. Sci. Soc. Amer. J.,* **74,** 1406–1425, doi:10.2136/sssaj2009.0288.

——, ——, ——, and ——, 2010b: Modeling the subsurface hydrology of Mer Bleue bog. *Soil. Sci. Soc. Amer. J.,* **74,** 680–694, doi:10.2136/sssaj2009.0148.

Dissanayaka, S. H., S. Hamamoto, K. Kawamoto, T. Komatsu, and P. Moldrup, 2012: Thermal properties of peaty soils: Effects of liquid-phase impedance factor and shrinkage. *Vadose Zone J.,* **11,** doi:10.2136/vzj2011.0092.

Dorsey, J. R., E. Nemitz, M. W. Gallagher, D. Fowler, P. I. Williams, K. N. Bower, and K. M. Beswick, 2002: Direct measurements and parametrisation of aerosol flux, concentration and emission velocity above a city. *Atmos. Environ.,* **36,** 791–800, doi:10.1016/S1352-2310(01)00526-X.

Dullien, F. A., 1991: *Porous Media: Fluid Transport and Pore Structure*. Academic Press, 574 pp.

Eichinger, W. E., M. B. Parlange, and H. Stricker, 1996: On the concept of equilibrium evaporation and the value of the Priestley–Taylor coefficient. *Water Resour. Res.,* **32,** 161–164, doi:10.1029/95WR02920.

Fairall, C. W., E. F. Bradley, D. P. Rogers, J. B. Edson, and G. S. Young, 1996: Bulk parameterization of air–sea fluxes for Tropical Ocean–Global Atmosphere Coupled–Ocean Atmosphere Response Experiment. *J. Geophys. Res.,* **101,** 3747–3764, doi:10.1029/95JC03205.

Falge, E., and Coauthors, 2001: Gap filling strategies for long term energy flux data sets. *Agric. For. Meteor.,* **107,** 71–77, doi:10.1016/S0168-1923(00)00235-5.

Finkelstein, P. L., and P. F. Sims, 2001: Sampling error in eddy correlation flux measurements. *J. Geophys. Res.,* **106,** 3503–3509, doi:10.1029/2000JD900731.

Flanagan, L. B., and K. H. Syed, 2011: Stimulation of both photosynthesis and respiration in response to warmer and drier conditions in a boreal peatland ecosystem. *Global Change Biol.,* **17,** 2271–2287, doi:10.1111/j.1365-2486.2010.02378.x.

Fraser, C., N. T. Roulet, and T. R. Moore, 2001: Hydrology and dissolved organic carbon biogeochemistry in an ombrotrophic bog. *Hydrol. Processes,* **15,** 3151–3166, doi:10.1002/hyp.322.

Froidevaux, M., and Coauthors, 2013: A Raman lidar to measure water vapor in the atmospheric boundary layer. *Adv. Water Resour.,* **51,** 345–356, doi:10.1016/j.advwatres.2012.04.008.

Grachev, A. A., E. L Andreas, C. W. Fairall, P. S. Guest, and P. O. G. Persson, 2007: SHEBA flux-profile relationships in the stable atmospheric boundary layer. *Bound.-Layer Meteor.,* **124,** 315–333, doi:10.1007/s10546-007-9177-6.

Halliwell, D. H., and W. R. Rouse, 1987: Soil heat flux in permafrost: Characteristics and accuracy of measurement. *J. Climatol.,* **7,** 571–584, doi:10.1002/joc.3370070605.

Hargreaves, G. H., and Z. A. Samani, 1982: Estimating potential evapotranspiration. *J. Irrig. Drain. Div.,* **108,** 225–230.

Heikinheimo, M., M. Kangas, T. Tourula, A. Venäläinen, and S. Tattari, 1999: Momentum and heat fluxes over lakes Tämnaren and Råksjö determined by the bulk-aerodynamic and eddy-correlation methods. *Agric. For. Meteor.,* **98-99,** 521–534, doi:10.1016/S0168-1923(99)00121-5.

Higgins, C. W., C. Meneveau, and M. B. Parlange, 2007: The effect of filter dimension on the subgrid-scale stress, heat flux, and tensor alignments in the atmospheric surface layer. *J. Atmos. Oceanic Technol.,* **24,** 360–375, doi:10.1175/JTECH1991.1.

Högström, U., 1988: Non-dimensional wind and temperature profiles in the atmospheric surface layer: A re-evaluation. *Bound.-Layer Meteor.,* **42,** 55–78, doi:10.1007/BF00119875.

Humphreys, E. R., P. M. Lafleur, L. B. Flanagan, N. Hedstrom, K. H. Syed, A. J. Glenn, and R. Granger, 2006: Summer carbon dioxide and water vapor fluxes across a range of northern peatlands. *J. Geophys. Res.,* **111,** G04011, doi:10.1029/2005JG000111.

Ingham, D. B., and I. Pop, 2002: *Transport Phenomena in Porous Media*. Vol. II. Elsevier, 450 pp.

Isabelle, P.-E., 2014: Simplification de l'estimation des taux d'évapotranspiration sur les tourbières boréales par la quasi-neutralité de l'atmosphère. M.S. thesis, Centre Eau Terre Environnement, Institut national de la recherche scientifique, Université du Québec, 202 pp.

Itier, B., and Y. Brunet, 1996: Recent developments and present trends in evaporation research: A partial survey. *Evapotranspiration and irrigation scheduling: Proceedings of the International Conference ASAE,* C. Camp, E. Sadler, and R. Yoder, Eds., 1–20.

Katul, G. G., and M. B. Parlange, 1992: A Penman–Brutsaert model for wet surface evaporation. *Water Resour. Res.,* **28,** 121–126, doi:10.1029/91WR02324.

Kellner, E., 2001: Surface energy fluxes and control of evapotranspiration from a Swedish sphagnum mire. *Agric. For. Meteor.,* **110** (2), 101–123, doi:10.1016/S0168-1923(01)00283-0.

Kim, J., and S. B. Verma, 1996: Surface exchange of water vapour between an open sphagnum fen and the atmosphere. *Bound.-Layer Meteor.,* **79,** 243–264, doi:10.1007/BF00119440.

Kleissl, J., S.-H. Hong, and J. M. Hendrickx, 2009: New Mexico scintillometer network: Supporting remote sensing and hydrologic and meteorological models. *Bull. Amer. Meteor. Soc.,* **90,** 207–218, doi:10.1175/2008BAMS2480.1.

Koerselman, W., and B. Beltman, 1988: Evapotranspiration from fens in relation to Penman's potential free water evaporation (E_o) and pan evaporation. *Aquat. Bot.,* **31,** 307–320, doi:10.1016/0304-3770(88)90019-8.

Kotani, A., and M. Sugita, 2005: Seasonal variation of surface fluxes and scalar roughness of suburban land covers. *Agric. For. Meteor.,* **135,** 1–21, doi:10.1016/j.agrformet.2005.09.012.

Lafleur, P. M., N. T. Roulet, J. L. Bubier, S. Frolking, and T. R. Moore, 2003: Interannual variability in the peatland–atmosphere carbon dioxide exchange at an ombrotrophic bog. *Global Biogeochem. Cycles,* **17,** 1036, doi:10.1029/2002GB001983.

——, R. A. Hember, S. W. Admiral, and N. T. Roulet, 2005: Annual and seasonal variability in evapotranspiration and water table at a shrub-covered bog in southern Ontario, Canada. *Hydrol. Processes,* **19,** 3533–3550, doi:10.1002/hyp.5842.

Leclerc, M. Y., R. H. Shaw, G. den Hartog, and H. H. Neumann, 1990: The influence of atmospheric stability on the budgets of the Reynolds stress and turbulent kinetic energy within and above a deciduous forest. *J. Appl. Meteor.,* **29,** 916–933, doi:10.1175/1520-0450(1990)029<0916:TIOASO>2.0.CO;2.

Liu, H. Z., J. W. Feng, L. Järvi, and T. Vesala, 2012: Four-year (2006–2009) eddy covariance measurements of CO_2 flux over an urban area in Beijing. *Atmos. Chem. Phys.,* **12,** 7881–7892, doi:10.5194/acp-12-7881-2012.

Mahrt, L., D. Vickers, J. Edson, J. M. Wilczak, J. Hare, and J. Højstrup, 2001: Vertical structure of turbulence in offshore flow during RASEX. *Bound.-Layer Meteor.,* **100,** 47–61, doi:10.1023/A:1018982828967.

Mauder, M., and T. Foken, 2011: Documentation and instruction manual of the eddy-covariance software package TK3. Tech. Rep., Universität Bayreuth, 60 pp.

Metzger, M., B. McKeon, and H. Holmes, 2007: The near-neutral atmospheric surface layer: Turbulence and non-stationarity. *Philos. Trans. Roy. Soc. London,* **A365,** 859–876, doi:10.1098/rsta.2006.1946.

Mölder, M., and E. Kellner, 2002: Excess resistance of bog surfaces in central Sweden. *Agric. For. Meteor.,* **112,** 23–30, doi:10.1016/S0168-1923(02)00043-6.

Monin, A. S., and A. M. Yaglom, 1971: *Statistical Fluid Mechanics*. Vol. I. MIT Press, 769 pp.

Monteith, J., 1965: Evaporation and environment. *The State and Movement of Water in Living Organisms,* G. E. Fogg, Ed., Symposia of the Society for Experimental Biology, Vol. 19, Cambridge University Press, 205–234.

Moriwaki, R., and M. Kanda, 2006: Scalar roughness parameters for a suburban area. *J. Meteor. Soc. Japan,* **84,** 1063–1071, doi:10.2151/jmsj.84.1063.

Nadeau, D. F., E. R. Pardyjak, C. W. Higgins, H. Huwald, and M. B. Parlange, 2013a: Flow during the evening transition over steep alpine slopes. *Quart. J. Roy. Meteor. Soc.,* **139,** 607–624, doi:10.1002/qj.1985.

——, A. N. Rousseau, C. Coursolle, H. A. Margolis, and M. B. Parlange, 2013b: Summer methane fluxes from a boreal bog in northern Québec, Canada, using eddy covariance measurements. *Atmos. Environ.,* **81,** 464–474, doi:10.1016/j.atmosenv.2013.09.044.

Nield, D. A., and A. Bejan, 2006: *Convection in Porous Media.* Springer-Verlag, 657 pp.

Novak, M., and T. Black, 1985: Theoretical determination of the surface energy balance and thermal regimes of bare soils. *Bound.-Layer Meteor.,* **33,** 313–333, doi:10.1007/BF00116682.

Novick, K. A., P. C. Stoy, G. G. Katul, D. S. Ellsworth, M. B. Siqueira, J. Juang, and R. Oren, 2004: Carbon dioxide and water vapor exchange in a warm temperate grassland. *Oecologia,* **138,** 259–274, doi:10.1007/s00442-003-1388-z.

Ochsner, T. E., T. J. Sauer, and R. Horton, 2007: Soil heat storage measurements in energy balance studies. *Agron. J.,* **99,** 311–319, doi:10.2134/agronj2005.0103S.

Oke, T. R., 1987: *Boundary Layer Climates.* Routledge, 435 pp.

Omstedt, A., L. Meuller, and L. Nyberg, 1997: Interannual, seasonal and regional variations of precipitation and evaporation over the Baltic Sea. *Ambio,* **26** (8), 484–492.

Paavilainen, E., and J. Päivänen, 1995: *Peatland Forestry: Ecology and Principles*. Springer, 253 pp.

Pagowski, M., 2006: An iterative solution of flux–profile relationships in the surface layer for regional model applications. *Atmos. Environ.,* **40,** 6892–6897, doi:10.1016/j.atmosenv.2006.07.027.

Park, S.-J., S.-U. Park, and C.-H. Ho, 2010: Roughness length of water vapor over land surfaces and its influence on latent heat flux. *Terr. Atmos. Ocean. Sci.,* **21,** 855–867, doi:10.3319/TAO.2009.11.13.01(Hy).

Parlange, M. B., W. E. Eichinger, and J. D. Albertson, 1995: Regional scale evaporation and the atmospheric boundary layer. *Rev. Geophys.,* **33,** 99–124, doi:10.1029/94RG03112.

Parmentier, F., M. Van der Molen, R. de Jeu, D. Hendriks, and A. Dolman, 2009: Fluxes and evaporation on a peatland in the Netherlands appear not affected by water table fluctuations. *Agric. For. Meteor.,* **149,** 1201–1208, doi:10.1016/j.agrformet.2008.11.007.

Penman, H. L., 1948: Natural evaporation from open water, bare soil and grass. *Proc. Roy. Soc. London,* **193A,** 120–145, doi:10.1098/rspa.1948.0037.

Petrone, R. M., J. S. Price, J. Waddington, and H. Von Waldow, 2004: Surface moisture and energy exchange from a restored peatland, Québec, Canada. *J. Hydrol.,* **295,** 198–210, doi:10.1016/j.jhydrol.2004.03.009.

——, U. Silins, and K. Devito, 2007: Dynamics of evapotranspiration from a riparian pond complex in the western boreal forest, Alberta, Canada. *Hydrol. Processes,* **21,** 1391–1401, doi:10.1002/hyp.6298.

Price, J. S., 1991: Evaporation from a blanket bog in a foggy coastal environment. *Bound.-Layer Meteor.,* **57,** 391–406, doi:10.1007/BF00120056.

Priestley, C., and R. Taylor, 1972: On the assessment of surface heat flux and evaporation using large-scale parameters. *Mon. Wea. Rev.,* **100,** 81–92, doi:10.1175/1520-0493(1972)100<0081:OTAOSH>2.3.CO;2.

Raddatz, R., T. Papakyriakou, K. Swystun, and M. Tenuta, 2009: Evapotranspiration from a wetland tundra sedge fen: Surface resistance of peat for land-surface schemes. *Agric. For. Meteor.,* **149,** 851–861, doi:10.1016/j.agrformet.2008.11.003.

Reichstein, M., and Coauthors, 2005: On the separation of net ecosystem exchange into assimilation and ecosystem respiration: Review and improved algorithm. *Global Change Biol.,* **11,** 1424–1439, doi:10.1111/j.1365-2486.2005.001002.x.

Roulet, N. T., P. M. Lafleur, P. J. Richard, T. R. Moore, E. R. Humphreys, and J. Bubier, 2007: Contemporary carbon balance and late Holocene carbon accumulation in a northern peatland. *Global Change Biol.,* **13,** 397–411, doi:10.1111/j.1365-2486.2006.01292.x.

Runkle, B., C. Wille, M. Gažovič, M. Wilmking, and L. Kutzbach, 2014: The surface energy balance and its drivers in a boreal peatland fen of northwestern Russia. *J. Hydrol.,* **511,** 359–373, doi:10.1016/j.jhydrol.2014.01.056.

Schwärzel, K., M. Renger, R. Sauerbrey, and G. Wessolek, 2002: Soil physical characteristics of peat soils. *J. Plant Nutr. Soil Sci.,* **165,** 479–486, doi:10.1002/1522-2624(200208)165:4<479::AID-JPLN479>3.0.CO;2-8.

——, J. Šimůnek, M. T. van Genuchten, and G. Wessolek, 2006: Measurement modeling of soil-water dynamics evapotranspiration of drained peatland soils. *J. Plant Nutr. Soil Sci.,* **169,** 762–774, doi:10.1002/jpln.200621992.

Shimoyama, K., T. Hiyama, Y. Fukushima, and G. Inoue, 2004: Controls on evapotranspiration in a west Siberian bog. *J. Geophys. Res.,* **109,** D08111, doi:10.1029/2003JD004114.

Silins, U., and R. L. Rothwell, 1998: Forest peatland drainage and subsidence affect soil water retention and transport properties in an Alberta peatland. *Soil. Sci. Soc. Amer. J.,* **62,** 1048–1056, doi:10.2136/sssaj1998.03615995006200040028x.

Sonnentag, O., G. Van der Kamp, A. Barr, and J. Chen, 2010: On the relationship between water table depth and water vapor and carbon dioxide fluxes in a minerotrophic fen. *Global Change Biol.,* **16,** 1762–1776, doi:10.1111/j.1365-2486.2009.02032.x.

Stull, R. B., 1988: *An Introduction to Boundary Layer Meteorology.* Springer, 670 pp.

Syed, K. H., L. B. Flanagan, P. J. Carlson, A. J. Glenn, and K. E. Van Gaalen, 2006: Environmental control of net ecosystem CO_2 exchange in a treed, moderately rich fen in northern Alberta. *Agric. For. Meteor.,* **140,** 97–114, doi:10.1016/j.agrformet.2006.03.022.

Tanny, J., S. Cohen, S. Assouline, F. Lange, A. Grava, D. Berger, B. Teltch, and M. Parlange, 2008: Evaporation from a small water reservoir: Direct measurements and estimates. *J. Hydrol.,* **351,** 218–229, doi:10.1016/j.jhydrol.2007.12.012.

Vercauteren, N., E. Bou-Zeid, M. B. Parlange, U. Lemmin, H. Huwald, J. Selker, and C. Meneveau, 2008: Subgrid-scale dynamics of water vapour, heat and momentum over a lake. *Bound.-Layer Meteor.,* **128,** 205–228, doi:10.1007/s10546-008-9287-9.

Verry, E., 1988: Hydrology of wetlands and man's influence on it. *Proc. of the Int. Symp. on the Hydrology of Wetlands in Temperate and Cold Regions,* Vol. 2, Joensuu, Finland, Academy of Finland National IHP Committee, 41–61.

Weiss, R., N. J. Shurpali, T. Sallantaus, R. Laiho, J. Laine, and J. Alm, 2006: Simulation of water table level and peat temperatures in boreal peatlands. *Ecol. Modell.,* **192,** 441–456, doi:10.1016/j.ecolmodel.2005.07.016.

Williams, C. A., and Coauthors, 2012: Climate and vegetation controls on the surface water balance: Synthesis of evapotranspiration measured across a global network of flux towers. *Water Resour. Res.,* **48,** W06523, doi:10.1029/2011WR011586.

Wu, J., L. Kutzbach, D. Jager, C. Wille, and M. Wilmking, 2010: Evapotranspiration dynamics in a boreal peatland and its impact on the water and energy balance. *J. Geophys. Res.,* **115,** G04038, doi:10.1029/2009JG001075.